Journal of Visualized Experiments

Longitudinal In Vivo Imaging and Quantification of Human Pancreatic Islet Grafting and Contributing Host Cells in the Anterior Eye Chamber

--Manuscript Draft--

Article Type:	Invited Methods Article - JoVE Produced Video
Manuscript Number:	JoVE61234R2
Full Title:	Longitudinal In Vivo Imaging and Quantification of Human Pancreatic Islet Grafting and Contributing Host Cells in the Anterior Eye Chamber
Section/Category:	JoVE Medicine
Keywords:	Diabetes Mellitus; Transplantation; pancreatic islet; human islet; anterior eye chamber; in vivo; Animal model; Longitudinal imaging; Post-transplantation; Revascularization; 2-Photon microscopy; image-based quantification
Corresponding Author:	Anja Schmidt-Christensen Lund University Malmö, Skåne SWEDEN
Corresponding Author's Institution:	Lund University
Corresponding Author E-Mail:	anja.schmidt-christensen@med.lu.se
Order of Authors:	Julia Nilsson
	Dan Holmberg
	Anja Schmidt-Christensen
Additional Information:	
Question	**Response**
Please indicate whether this article will be Standard Access or Open Access.	Standard Access (US$2,400)
Please indicate the **city, state/province, and country** where this article will be **filmed**. Please do not use abbreviations.	Lund, Skåne, Sweden

TITLE:

Longitudinal In Vivo Imaging and Quantification of Human Pancreatic Islet Grafting and Contributing Host Cells in the Anterior Eye Chamber

AUTHORS AND AFFILIATIONS:

Julia Nilsson[1,2], Dan Holmberg[1,2], Anja Schmidt-Christensen[1,2]

[1]Department of Experimental Medical Science, Lund University, Sweden
[2]Lund University Diabetes Centre, Malmö, Sweden

Corresponding Author:

Anja Schmidt-Christensen (anja.schmidt-christensen@med.lu.se)

Email Addresses of Co-authors:

Dan Holmberg (dan.holmberg@med.lu.se)
Julia Nilsson (Julia.nilsson@med.lu.se)

KEYWORDS:

diabetes mellitus, transplantation, pancreatic islets, human islet, intraocular, anterior eye chamber, in vivo imaging, animal model, longitudinal imaging, posttransplantation, revascularization

SUMMARY:

The goal of this protocol is to continuously monitor the dynamics of the human pancreatic islet engraftment process and the contributing host versus donor cells. This is accomplished by transplanting human islets into the anterior chamber of the eye (ACE) of an NOD.(Cg)-*Gt(ROSA)26Sor*^{tm4}-*Rag2*$^{-/-}$mouse recipient followed by repeated 2-photon imaging.

ABSTRACT:

Imaging beta cells is a key step towards understanding islet transplantation. Although different imaging platforms for the recording of beta cell biology have been developed and utilized in vivo, they are limited in terms of allowing single cell resolution and continuous longitudinal recordings. Because of the transparency of the cornea, the anterior chamber of the eye (ACE) in mice is well suited to study human and mouse pancreatic islet cell biology. Here is a description of how this approach can be used to perform continuous longitudinal recordings of grafting and revascularization of individual human islet grafts. Human islet grafts are inserted into the ACE, using NOD.(Cg)-*Gt(ROSA)26Sor*^{tm4}-*Rag2*$^{-/-}$mice as recipients. This allows for the investigation of the expansion of recipient versus donor cells and the contribution of recipient cells in promoting the encapsulation and vascularization of the graft. Further, a step-by-step approach for image analysis and quantification of the islet volume or segmented vasculature and islet capsule forming recipient cells is outlined.

INTRODUCTION:

Diabetes mellitus describes a group of metabolic diseases characterized by elevated levels of

blood glucose as results of insufficient insulin production from loss or dysfunction of pancreatic islet beta cells, often accompanied by insulin resistance. Type 1 (T1D) and type 2 diabetes (T2D) are complex diseases in which the progressive dysfunction of the beta cells causes disease development. T1D is precipitated by an autoimmune attack on the beta cells, while T2D is considered to be driven by metabolic factors, albeit with increasing evidence of low-grade systemic inflammation[1]. Transplantation of donor human islets, particularly to T1D patients, offers the potential for providing physiological glycemic control. However, a shortage of tissue donors and poor islet engraftment has prevented islet transplantation to become a mainstream therapeutic option. A substantial proportion of the functional islet graft is lost in the immediate posttransplantation period (24–48 h) due to the hypoxic, inflammatory, immunogenic host environment[2,3]. To evaluate the efficiency of intervention methods for the improvement of islet survival, continuous monitoring of such transplantations is necessary.

In vivo techniques to image and track the fate of transplanted human pancreatic islets after transplantation still remains a challenge for diabetes research[4,5]. To date, noninvasive imaging techniques, including positron emission tomography (PET), magnetic resonance imaging (MRI), or ultrasound (US) show potential for the quantification and functional evaluation of transplanted islets in experimental conditions[5]. However, given the small islet sizes, quantitative measurements by those modalities suffer from insufficient resolution. The anterior chamber of the eye (ACE) as a transplantation site for observation is a promising noninvasive imaging solution offering effectively higher spatial resolution and frequent monitoring over long time periods[6]. This method has been successfully exploited to study mouse islet biology (reviewed in Yang et al.[7]), autoimmune immune responses[8], as well as human islet grafting[9,10].

Here the ACE transplantation method is combined with a 2-photon imaging approach to investigate the dynamics of the human pancreatic islet engraftment process by continuous and repeated recordings on individual islet grafts for up to 10 months after transplantation. The multiphoton imaging properties of greater imaging depths and reduced overall photobleaching and photo damage overcome the imaging limitations of confocal microscopy[11]. Quantification of fluorescent imaging involves several stages, including islet sample preparation, islet transplantation, image acquisition, image filtering to remove islet noise or background, segmentation, quantification, and data analysis. The most challenging step is usually partitioning or segmenting an image into multiple parts or regions. This could involve separating signal from background noise, or clustering regions of voxels based on similarities in color or shape to detect and label voxels of a 3D volume that represents islet vasculature, for example. Once segmented, statistics such as object volume sizes are typically straightforward to extract. Provided is a method for the quantification and extraction of the imaging data, such as segmentation and data visualization. Particular attention is paid to the removal of autofluorescence in human islets and distinction between islet vasculature and islet capsule forming recipient cells.

PROTOCOL:

The Regional Ethics Committee in Lund, Sweden, approved the study according to the Act Concerning the Ethical Review of Research Involving Humans. Animal experiments were

performed in strict accordance with the Swedish ethics of animal experiments and approved by the ethics committees of Malmö and Lund. Six to 8-week-old immunodeficient NOD.(Cg)-*Gt(ROSA)26Sor*^{tm4}-*Rag2*$^{-/-}$ (NOD.*ROSA*-tomato.*Rag2*$^{-/-}$) recipient mice were used as recipients for transplantation of human islets[10].

1. Islet preparation for transplantation

1.1. Culture human islets in CMRL 1066 supplemented with 10 mM HEPES, 2 mM L-glutamine, 50 µg/mL gentamycin, 0.25 µg/mL fungizone, 20 µg/mL ciproxfloxacin, 10 mM nicotinamide (NIC), and 10% heat-inactivated human serum at 37 °C in 5% CO_2 and humidified air until transplantation, as described previously[12].

NOTE: Islets should be free of exocrine tissue and not touch each other in culture. Exocrine tissues appear translucent.

1.2. On the day of transplantation, transfer culture media containing the islets to a new Petri dish using an aspirator tube assembly connected to a pulled glass capillary.

NOTE: Alternatively, use a 200 µL pipette. Coloring the back of the Petri dish helps make the islets more easily distinguishable under the stereo microscope.

1.3. Using a stereo microscope, pick ~20–40 islets per transplantation and transfer to a 1.5 mL tube. Fill the tube to the top with culture media from the incubator.

1.4. Seal the tubes with paraffin film and store on ice until transplantation. Prepare an appropriate amount for the number of transplantations performed.

1.5. Alternatively, ensure a CO_2 incubator is available in the surgery room to keep islets in culture and pick them immediately prior to each transplantation.

2. Preparation of transplantation equipment and surgery table

NOTE: All surgical tools should be autoclaved, and the surgery table and instruments disinfected with 70% alcohol.

2.1. Connect a stereotaxic head holder to anesthesia via a nose mask and turn on the heating pad.

2.2. Connect a gastight Hamilton syringe to polyethylene tubing and a blunt end eye cannula.

NOTE: It is recommended to fill all parts with PBS before assembly. Check for trapped air bubbles and remove if present.

2.3. Attach the Hamilton syringe tightly to the table (**Figure 1a**) or a movable base (**Figure 1e**)

and attach the tubing to the stereo microscope, with cannula hanging down (i.e., waiting position).

NOTE: Use surgical tape, because it is easy to remove and reattach.

2.4. Prepare a 1 mL syringe connected to a 30 G needle filled with 0.1 mg/kg buprenorphine solution.

2.5. Prepare a syringe with sterile PBS for the eye. Alternatively, use a pipette.

2.6. Set aside a clean wake up cage with heating lamp.

3. Anesthesia and positioning of recipient mice for surgery

NOTE: All animals were bred and maintained in a pathogen-free environment at the animal facilities at Lund University.

3.1. Anesthetize the mouse in a chamber filled with 40% O_2/60% N_2/3% isoflurane and transfer the anesthetized mouse to the head holder platform on a warm heating pad (**Figure 1a**). Check for the lack of pedal reflexes.

NOTE: Isoflurane anesthesia is the preferred method of anesthesia for fast recovery after surgery. The microscope room must be properly ventilated to use isoflurane.

3.2. Place the snout of the mouse into the anesthesia mask connected to 40% O_2/60% N_2/0.9%–1.5% isoflurane anesthesia machine. Use the thumb and finger to lift the head up slightly and fasten it using the metallic pieces on the sides. Ensure that the earpieces fix the head directly below the ears. Inject 0.1 mg/kg buprenorphine solution subcutaneously on the back of the mouse.

NOTE: Buprenorphine is used as an analgesic.

3.3. Tilt the head so that the eye to be operated on is facing upwards and is close to the researcher.

3.4. Gently retract the eyelids of the eye to be transplanted using blunt forceps, pop the eye out, and loosely fix with a pair of tweezers. Ensure that the tips of the tweezers are covered with a polythene tube attached to the head holder platform (**Figure 1a**, insert).

3.5. Always keep both eyes wet by applying a droplet of sterile PBS onto the eye.

3.6. Transfer the human islets from the culture plate (section 1) to a Petri dish with sterile PBS and make sure that the islets are close to each other to minimize the amount of cell culture media transferred (**Figure 1c**).

3.7. Pick up ~20–30 islets in the eye cannula connected via polythene tubing to the Hamilton syringe.

NOTE: Take up as little liquid as possible with the islets.

3.8. Hang the tubing upside down and attach to the stereo microscope (**Figure 1d**). Tape the tubing carefully to let the islets sink to the end of the tube toward the cannula.

4. Transplantation procedure

NOTE: This method has been previously described for the transplantation of mouse islets[6]. A slightly modified procedure is presented here.

4.1. Pinch the pads on the hind legs to make sure that the mouse is asleep.

4.2. Tighten the forceps restraining the eye without disrupting the blood flow and apply a droplet of sterile PBS onto the eye.

4.3. Using a 25 G needle as a scalpel, bevel upwards, carefully penetrate only half of the tip in the cornea and make a single lateral incision. Make the hole in an upward angle; the hole will seal more easily after the transplant (**Figure 1f**).

4.4. Carefully lift up the cornea with the cannula preloaded with islets and slowly apply islets in the eye. Slowly retract the cannula from the ACE. Avoid insertion of the cannula into the anterior chamber to prevent damage of the iris, but rather push carefully against the corneal opening (**Figure 1g**).

NOTE: Aim for an injection volume of 3–8 µL. If the volume is too large, it will expose the eye to unnecessarily high intraocular pressure and may result in reflux of the injected islets out of the anterior chamber.

4.5. When facing difficulties with insertion of the islets due to increased pressure in the eye chamber, enlarge the incision site by reinforcing the lateral incision site and reapply islets.

NOTE: Occasionally, introduced air bubbles can be used as space holders. The bubbles will disappear on their own.

4.6. Apply eye gel to the eye, loosen the eye-restraining forceps and leave the mouse on isoflurane in the same position for 8–10 min to let the islets set.

4.7. Remove the forceps holding the eyelid and put the eyelid back to its normal position.

4.8. Remove the mouse from the head holder and transfer it to a wake up cage.

4.9. When the mouse is awake and moving, transfer it back to the original cage and keep in the animal housing until scanning (at least 5 days are recommended).

5. Imaging of implanted human islets by 2-photon microscopy

NOTE: Taking overview images of the eye using a fluorescence stereoscopic microscope (**Figure 2a**–**c**) 4–5 days after transplantation prior to 2-photon imaging is recommended to localize the islets of interest. Avoid restraining the eye too tightly this early after transplantation. Use 2-photon imaging 6–7 days posttransplantation.

5.1. Start the image acquisition software (see **Table of Materials**). In the "**Laser**" menu activate the Mai Tai laser (Power "**ON**") and in the "**Light Path**" menu set the wavelength to 900 nm and apply a minimal transmission laser power starting with 5%–10% laser power (use sliders).

NOTE: While scanning, adjust the laser power as needed.

5.2. Set green, orange, and red channels. Collect emission light simultaneously onto three nondescanned detectors (NDD) using a dichronic mirror (LBF 760) and emission filter information as follows: Red/Angiosense 680, 690–730 nm; Green/Autofluorescence, 500–550 nm; and Orange/Tomato, 565–610nm (**Figure 2d**).

5.3. Place the head holder stage onto the motorized microscope stage and connect the gasmask to the tubing of the anesthesia machine and tubing connected to ventilation system. Turn on the heating pad.

5.4. Anesthetize the recipient mouse, transfer to the head holder platform, restrain the eye for imaging, and administer buprenorphine solution as described above (steps 3.1–3.5).

5.5. Adjust isoflurane vapors as needed. A breath rate of ~55–65 breaths per minute (bpm) indicates optimal anesthesia. If anesthesia is too deep, the rate will be <50 bpm with heavy breathing or gasping; if too light, the rate will be >70 bpm with superficial breathing. Carefully monitor mice during anesthesia by visual inspection every 15 min.

NOTE: Anesthetization varies from mouse to mouse, between mouse strains, and as time under anesthesia progresses[13].

5.6. Administer enough eye gel onto the eye as an immersion liquid between the cornea and the lens, allowing it to slowly accumulate (**Figure 2f**, insert). Avoid air bubbles.

NOTE: Side illumination with a flexible metal hose lamp is recommended to adjust the focus and localize islet grafts.

5.7. To visualize blood vessels, administer 100 µL of the imaging agent (e.g., Angiosense 680)

intravenously into the tail vein using a disposable insulin 30 G syringe.

5.8. In "**Acquisition mode**" adjust the frame size to 512 x 512 and the scan speed.

NOTE: Slower scans (i.e., increasing dwell time) will improve the signal-to-noise ratio.

5.9. In the "**Channels**" menu adjust **Master Gain** for each PMT in Volts to amplify the signal until an image is seen on screen in the **Live** scanning mode. The higher this value, the more sensitive the detector becomes to signal and noise.

NOTE: Preferably, keep values between 500–800 V.

5.10. In the "**Z-stack**" menu define the beginning and the end of the z-stack by manually moving the focus to the top of the islet graft. Save position by selecting "**Set First**". Move to the last bottom plane that can be focused in the islet graft and save position by selecting "**Set Last"**. Use a z-step size of 2 µm.

5.11. Collect the final image stack by clicking the "**Start Experiment**" tab and save as 8-bit CZI (i.e., Carl Zeiss format) file.

6. Imaging of implanted human islets by confocal microscopy

NOTE: The total volume, morphology, and plasticity of transplanted islets can be assessed by monitoring the in vivo scattering signal in a separate scan (i.e., separate track) by detection of laser backscatter light[10].

6.1. Take out the main beam splitter (i.e., LBF Filter) and in the "**Light Path**" dialog set up a separate track for confocal imaging. Choose the Argon laser with wavelength of 633 nm and detection at the same wavelength as the laser light. Z-stacks are acquired with a step size of 2–3 µm for backscatter light signal.

6.2. Readjust the z-stack settings to make sure to record the whole islet (see step 5.10).

6.3. Acquire image stack save as 8 bit CZI file.

7. Image analysis

NOTE: Commercial software (see **Table of Materials**) was used for this step.

7.1. Removing islet autofluorescence (**Figure 3b**)

7.1.1. In the "**Image processing**" tab choose "**Channel arithmetic´s**" and type "**ch1-ch2**". This creates a new channel 4 (ch 4); rename as "Vasculature".

NOTE: The Green/Autofluorescence channel is subtracted from Red/Angiosense channel.

7.1.2. Repeat the previous step and type "**ch3-ch2**" to create a new channel (ch 5); rename as "**Tomato** (**all**)".

NOTE: The Green/Autofluorescence channel is subtracted from the Orange/Tomato channel.

7.2. Defining islet mask by manual drawing (**Figure 3c**)

7.2.1. Create a new surface (blue symbol) and in the wizard choose "**Edit manually**". Keep the pointer in "**Select**" mode and in 3D view unclick "**Volume**" (under **Scene**) to visualize sections.

7.2.2. For easier islet border discrimination, activate all channels, including ch 1–ch 3.

NOTE: The Orange/Tomato channel is useful to define islet borders by the Tomato capsule signal. Alternatively, increase channel intensities to use multichannel islet autofluorescence and detector background signal as guidance.

7.2.3. In the "**Drawing**" tab choose "**Contour**" and click "**Draw**" to start drawing contours around the islet border starting in slice position 1.

7.2.4. Move to a new slice position and repeat drawing contours. Finish with the last slice on the top of the islet and end by clicking the "**Create surface**" tab. Usually it is enough to draw contours every 10^{th} slice.

7.3. Segmentation of "**Islet vasculature**" and "**Islet tomato**" fluorescence using islet mask (**Figure 3d**).

7.3.1. Choose the previously defined "**Islet mask**" object, go to the editing tab (**pencil** symbol), and click the "**Mask all**" tab, which opens a new window.

7.3.2. Choose the previously named channel "**Vasculature**" (ch 4) in the channel selection dropdown menu and activate options "**Duplicate channel before applying mask**", "**Constant inside/outside**", and set voxels outside surface to "**0.000**", which creates a new channel; rename as "**Islet vasculature**" (ch 6).

7.3.3. Repeat steps 7.3.1 and 7.3.2 and choose the previously created channel "**Tomato** (**all**)" (ch 5) in the channel selection drop down menu to create the new channel; rename as "**Islet tomato**" (ch 7).

7.4. Surface rendering of islet vasculature (**Figure 3e**)

7.4.1. Create a new surface in the "**Scene**" menu and in the wizard choose "**Automatic creation**".

7.4.2. Set the source channel to previously created "**Islet vasculature**" (ch 6) and choose background subtraction. Automatic threshold estimation can be adjusted if needed. Compare to the responding fluorescence channel (e.g., by blending in/out the newly created surface tab). Proceed in the wizard.

7.4.3. Optionally, use filters. For example, choose "**Volume**" and adjust the filter (yellow) in the window, which can remove selected surface objects. Finish the wizard and name the new surface object "**Islet vasculature**".

7.5. Segmentation of "**Islet tomato vasculature**" fluorescence signal (**Figure 3f**)

7.5.1. In the previously created "**Islet vasculature"** surface object, go to editing tab and click the "**Mask all**" tab, which opens a new window.

7.5.2. Choose the previously named channel "**Islet tomato**" (ch 7) in the channel selection drop down menu and set voxels outside surface to "**10.000**", which creates the new channel; rename as "**Islet tomato vasculature**" (ch 8).

7.6. Segmentation of "**Tomato capsule**" fluorescence signal (**Figure 3g**)

7.6.1. Choose "**Channel Arithmetic's**" in the "**Image processing**" tab and type "**ch7-ch8**", creating the new channel; rename as "**Tomato capsule**" (ch 9).

NOTE: The "**islet tomato vasculature**" fluorescence signal is subtracted from the total "**islet tomato**" fluorescence signal.

7.7. Surface rendering of "**Islet tomato vasculature**" and "**Tomato capsule**" (**Figure 3h**)

7.7.1. Follow step 7.4, and in the wizard choose source channels "**Islet tomato vasculature**" (ch 8) or "**Tomato capsule**" (ch 9) to create new surface objects accordingly.

7.8. Surface rendering of total islet surface (**Figure 3i**)

7.8.1. Open the islet backscatter file and create a new surface.

7.8.2. In the wizard, choose "**Automatic creation**" and define "**Region of interest**".

NOTE: "**Region of interest**" is used to separate the signals of multiple islets and to define the depth of the islet to be analyzed (e.g., top 75 µm).

7.8.3. In "**Absolute intensity**" adjust threshold if needed. The surface object can be clicked on or off to cross-check with corresponding channel intensity. Close the wizard.

7.9. Quantification (**Figure 3j**)

7.9.1. Select a created surface object in the "**Scene**" menu and go to the "**Statistics**" tab.

7.9.2. To retrieve detailed volume data in the selected surface object choose the "**Detailed**" tab and select "**Specific values**" and "**Volume**" from dropdown menu. To retrieve a total volume value of the selected surface object, go to the "**Detailed**" tab and choose "**Average values**".

REPRESENTATIVE RESULTS:

Non-labeled human islets were transplanted into the ACE of 8-week-old female NOD.(Cg)-*Gt(ROSA)26Sor*^{tm4}-*Rag2*$^{-/-}$(NOD.*ROSA*-tomato.*Rag2*$^{-/-}$) recipient mice. To prevent human tissue rejection, immunodeficient Rag2 knockout mice were chosen as recipients. In these transgenic mice, all cells and tissues expressed a membrane-targeted tomato fluorescence protein (mT) that allows clear identification of the recipient and the donor tissue. Repeated imaging of islet grafts by high-resolution 2-photon microscopy could identify mT^{+} recipient cells involved in the engraftment process and their dynamic migration pattern.

In general, the transplantation setup of human islets into the ACE of the recipient mice (**Figure 1a**) was similar to syngeneic mouse islet transplantations with regard to islet shape and size (**Figure 1b**,**c**). **Figure 1d**,**e** shows a typical transplantation with a detailed schematic showing the lateral incision site (**Figure 1f**) and dispersion of islets into the eye chamber (**Figure 1g**) and a representative outcome of injected mouse islets (**Figure 1h**) or human islets (**Figure 1i**). The grafting rate of human islets was generally lower (~30%) than that of mouse islets (50–70%). A possible reason for this discrepancy is that the availability of human islets is unpredictable, usually with only a 1 day notice, and also that the obtained islets vary in donor age, donor BMI, purity (45%–86%), and postisolation culture time (2–5 days). In contrast, islet isolations from mice can be easily planned. These were isolated from 6–8-week-old (i.e., young adult) mice with high purity and short, overnight culture times. These discrepancies between mouse and human islet grafts should be considered when interpreting the results.

In vivo fluorescence imaging of human islet grafts was compromised by significant interference from tissue autofluorescence (**Figure 4**). The visualization of the revascularization process of ACE-transplanted human islet grafts by imaging agents using traditional wavelengths in the visible spectrum was hampered by a low signal-to-noise ratio and high level of natural islet autofluorescence, illustrated by images of a λ-scan in the spectral range of 500–700 nm (**Figure 4a**) or by the sensitive nondescanned PMT detector with filter for detection of dextran TR (610–675 nm) (**Figure 4b**). This high background was not observed in mouse islet grafts (**Figure 4c**). The NIR emitting imaging agent Angiosense 680 showed a visibly higher signal-to-background ratio due to decreases in background noise in the NIR range 690–730 nm (**Figure 4d**, **Figure 3a**). The additional recording of an "unused" channel (i.e., 500–550 nm) could be used in a later image processing step to remove remaining background noise caused by natural islet autofluorescence. The 2-photon/confocal imaging setup (**Figure 2d–f**) is similar to previously described ones[6], save for the use of 900 nm 2-photon excitation and fluorescence detection of Angiosense 680, autofluorescence, and tomato channels with nondescanned PMTs 1-3 (**Figure 2d**). It is advisable

to measure the laser output power reaching the sample for each microscope setup (**Figure 2e**). Further, it is recommended to initially image the grafted islets with stereomicroscopy (**Figure 2a–c**), which will help select islets of interest and avoid 2-photon microscopy images of an unsuccessful transplantation.

The purpose of extracting quantitative data from many images was to remove potential bias in data selection and to obtain the statistical power necessary to detect a legitimate effect when comparing experiments. Quantification from fluorescent imaging of pancreatic islets involved several steps, each of which may have influenced the results in another. Here, interactive imaging software was used. It contains features allowing visualization of volume images and objects and identification of objects according to their morphology or intensity. **Figure 3** illustrates the different steps in image segmentation. The removal of autofluorescence by subtraction of the "autofluorescence" channel improved the signal-to-noise ratio (**Figure 3a**,**b**). The islet boundary called "islet mask" (**Figure 3c**) and corresponding channels (**Figure 3d**) was defined manually. The segmentation of the tomato signal into the islet vasculature and islet capsule (**Figure 3f**,**g**) and final surface rendering (**Figure 3e**,**h**,**i**) was used to extract quantitative data.

Figure 5 shows a representative longitudinal imaging session of the same human islet graft at 2 weeks, 2 months, 5 months, and 8 months posttransplantation into the ACE of a NOD.*ROSA*-tomato.*Rag2*$^{-/-}$ recipient mouse. Illustrated are maximum intensity projections (MIP) images of originally recorded RAW data (**Figure 5a**), processed images after islet autofluorescence removal (**Figure 5b–e**, **f–i**), and segmented islet objects including capsule (**Figure 5j-m**) or islet vasculature forming *mT*$^{+}$ recipient cells (red, **Figure 5n–q**) and total islet vasculature (green, **Figure 5n–q**).

FIGURE AND TABLE LEGENDS:

Figure 1: Transplantation of pancreatic islets into the anterior chamber of the eye. (**a**) Transplantation setup showing anesthetized mouse fixed in stereotaxic head holder and the exposed eye (inset) next to the prepared Hamilton syringe fixed to the table and the stereomicroscope ready to pick mouse islets (**b**) or human islets (**c**). (**d**) Waiting position of the eye cannula loaded with islets. (**e**) Transplantation in process, and (**f**) schematic drawing of a single lateral incision used to carefully lift up the cornea with the tip of the eye cannula and dispense islets into the anterior chamber (**g**). Image of the eye immediately after injection of mouse islets (**h**) or human islets (**i**). Scale bar = 500 µm.

Figure 2: Imaging of ACE-implanted pancreatic islet grafts. (**a**) Experimental fluorescent stereo microscope imaging setup. Widefield (**b**) or fluorescent image (**c**) of B6.*ROSA*-tomato islet grafts. (**d**) Simplified scheme of the emission light path. LBF: Laser-blocking filter (main beam splitter); LP: Long pass; BP: Band pass; PMT: Photomultiplier. (**e**) Laser output power depends strongly on the wavelength. Diagram shows actual laser output power in Watts (W) related to the power level of the laser beam (%), measured for the microscope setup. Circle: 800 nm, square: 900 nm, triangle: 1,000 nm. (**f**) Experimental imaging setup showing the recipient mouse with ACE-grafted islets (insert) mounted onto the motorized stage a commercial microscope. Scale bar = 100 µm

Figure 3: **Image segmentation of a human islet grafted in the ACE of a NOD.*ROSA*-tomato.*Rag2*$^{-}$**

$^{-/-}$ **recipient mouse.** (**a**) Original recording: Shown is a 3D rendering of an image stack of a human islet with merged channels or optical sections of split channels Angiosense 680 (ch 1), autofluorescence (ch 2), and tomato (ch 3). (**b**) 3D rendering of image stack with merged channels or optical sections with split channels "**Vasculature**" (ch 4) and "**Tomato(all)**" (ch 5) after autofluorescence removal. (**c**) Islet mask (yellow). (**d**) 3D rendering of image stack with merged or split channels "**islet vasculature**" (ch 6, white), "**islet tomato**" (ch 7, red). (**e**) Surface object "**islet vasculature**" created from ch 6. (**f**) 3D rendering of image stack with merged channels "**islet vasculature**" (ch 6, green) and "**islet tomato vasculature**" (ch 8, red). (**g**) 3D rendering of "**tomato capsule**" (ch 9) after channel subtraction ch 7–ch 8 or optical section with merged channels "**tomato capsule**" (ch 9, white), islet tomato vasculature (ch 8, red), and islet vasculature (ch 6, green). (**h**) Surface rendering of tomato capsule (created from ch 9) and islet tomato vasculature (created from ch 8). (**i**) Islet segmentation from human islet backscatter signal showing the selection of "**Region of interest**"(left) and the segmented surface object (middle) compared to the channel intensity (right). (**j**) Retrieval of data from the statistics tab. Scale bar = 50 µm.

Figure 4: Autofluorescence of human islets. Human islets (**a**,**b**,**d**) or B6 mouse islets (**c**) were transplanted into the ACE of NOD.*Rag2*$^{-/-}$ or B6 recipient mice and injected with dextran TR (**a**–**c**) or Angiosense 680 imaging agent (**d**) for the visualization of blood vessels. (**a**) λ-scan of human islet graft at the range from 500–700 nm with 2-photon excitation at 900 nm. Maximum image projection (MIP) image of human (**b**) or mouse islet graft (**c**) excited at 900 nm and detected with the TR filter (610–675 nm) of the NDD. (**d**) MIP of a human islet graft excited at 900 nm and detection with the Angiosense 680 filter (690–730 nm) of the NDD. Scale bar = 50 µm.

Figure 5: **Transplanted human islets are progressively revascularized and encapsulated by mT expressing cells of recipient origin.** Human islets transplanted into the anterior eye chamber of NOD. *ROSA*-tomato.*Rag2*$^{-/-}$ recipient mice, were imaged repeatedly for up to 8 months. Angiosense 680 was injected for the visualization of vasculature. (**a**) Maximum intensity projections (MIP) of original recorded RAW data of split (vasculature, autofluorescence, mT) or merged channels and backscatter light signal at 5 months posttransplantation. MIPS of total vasculature alone (**b**–**e**) or merged with membrane-targeted tomato fluorescence (mT) (**f**–**i**) after islet autoflourescence removal (green, **a**). 3D renderings of segmented islet tomato capsule (**j**–**m**) and islet tomato vasculature (red) or total islet vasculature (green) (**n**–**q**) at indicated time points posttransplantation. Scale bar = 50 µm.

DISCUSSION:

A method is presented to study the human pancreatic islet cell grafting process by observing the involvement of recipient and donor tissue. After a minimal invasive surgery implanting human islets into the anterior chamber of an immunodeficient mouse eye, the mouse recovers quickly within minutes after surgery. The procedure is performed on one eye. Generally, from 5–7 days postimplantation onwards the cornea is sufficiently healed to perform intravital imaging.

In this protocol, the quality of the human islet grafts is critical. Human islet quality and thereby transplantation outcome can vary depending on the donor's age, BMI, and isolation process, as well as time of islet culture prior to and after arrival. Human islets processed from organ donor

pancreases approved for clinical transplantation and research purposes were used with consent of the donors. They were obtained after a process of pancreas digestion and islet purification described elsewhere[12]. Similar to isolated murine islets, these islets undergo a number of cellular assaults such as ischemia, mechanical stress, loss of basement proteins, and partial disruption of intra-islet endothelial cells (ECs) during the enzymatic digestion step[14,15]. Despite constantly improving culture conditions and recovery of large numbers of high-quality human islets, the time to transplantation remains a critical factor. During the first days of culture, human islets show a significant loss of intra-islet ECs and upon 6 days of culture only small endothelial structures in the islet core can be detected[16]. This loss of intra-islet endothelial cells could constitute a critical factor in the reduced grafting of human islets, because donor islet ECs are important players in the revascularization process[17].

Maintaining sterility during the transplantation procedure is critical to avoid eye infections in the immunocompromised NOD.*ROSA*-tomato.*Rag2*$^{-/-}$ mice. Typically, transplantation procedures are performed under clean conditions using gloves, lab coat, head cover, and mouth mask, but not inside a biosafety cabinet. All used solutions are sterile filtered, and syringes, cannula, tubing, and gauze are rinsed in 70% ethanol. Wake-up cages are autoclaved. While full sterility cannot be guaranteed because of manual handling of the mouse during the procedure, islet contamination or eye infections have not been issues with this procedure.

Stable and adequate anesthesia is an important and critical factor for reducing eye movements and drift during low framerate data acquisition, and effectiveness can vary between different anesthetic agents[18]. Under light, general isoflurane anesthesia, the eye occasionally moves in a slow rolling fashion and increased depth of anesthesia (from 1–2%) can generally reduce eye movements. The clear advantage of using inhalable anesthesia is its quick effect and recovery time. It should be pointed out, however, that the use of isoflurane may alter insulin secretion[19].

Image analysis and segmentation, or the partitioning of an image into multiple regions, are challenging and subject to potential bias in data selection[20]. Segmentation aims to identify objects like the “islet vasculature” for quantification. Here, methods based on intensity-threshold were applied to select regions (i.e., “absolute intensity”) or intensity differences to find edges (i.e., “background subtraction”). Currently, there are no universal solutions for segmentation in fluorescent microscopy. One approach is to experiment with commercial software that supports a range of methods. If thresholding fails because of background intensity variation, then small changes in image capture settings may improve segmentation results.

A limitation of the method lies in the fact that the human graft is more rapidly replaced by recipient cells and, in fact, completely reconstituted by mouse recipient endothelial cells. This would preclude studies of human cell interactions if the aim is to study adoptively transferred human immune cells migrating into the islet parenchyma via interactions with human endothelial cells, for example. However, both in mouse and human islet grafts, similar revascularization occurs from the recipient and follows the different anatomical 3D plan specific for the species.

The success rates of beta cell replacement therapy have continued to improve. Still, various

challenges in evaluating the efficiency of islet grafting and survival in vivo remain unresolved due to the lack of appropriate intravital imaging technologies. The anterior eye chamber is a useful transplantation site, supporting the repeated and long-term in vivo imaging of islet cells for the study of islet morphology, vascularization patterns, beta cell function, and beta cell death at a cellular resolution.

The protocol for studying the grafting process of human islet transplants in the ACE transplantation site reported here allows for longitudinal monitoring of human islets grafts with considerably higher resolution than that obtained with other alternative longitudinal platforms such MRI [21,22], PET [23], SPECT[24], or Bioluminescence[25].

ACKNOWLEDGMENTS:

This study was supported by the Swedish Research Council, Strategic Research Area Exodiab, Dnr 2009-1039, the Swedish Foundation for Strategic Research Dnr IRC15-0067 to LUDC-IRC, the Royal Physiographic Society in Lund, Diabetesförbundet and Barndiabetesförbundet.

DISCLOSURES:

The authors have nothing to disclose.

REFERENCES:

1. Kharroubi, A. T., Darwish, H. M. Diabetes mellitus: The epidemic of the century. *World Journal of Diabetes.* **6** (6), 850-867 (2015).
2. Kanak, M. A. et al. Inflammatory response in islet transplantation. *International Journal of Endocrinology.* **2014**, 451035 (2014).
3. Nanji, S. A., Shapiro, A. M. Advances in pancreatic islet transplantation in humans. *Diabetes, Obesity, Metabolism.* **8** (1), 15-25 (2006).
4. Malaisse, W. J., Maedler, K. Imaging of the beta cells of the islets of Langerhans. *Diabetes Research and Clinical Practice.* **98** (1), 11-18 (2012).
5. Kim, D., Jun, H. S. In Vivo Imaging of Transplanted Pancreatic Islets. *Frontiers in Endocrinology.* **8**, 382 (2017).
6. Speier, S. et al. Noninvasive high-resolution in vivo imaging of cell biology in the anterior chamber of the mouse eye. *Nature Protocols.* **3** (8), 1278-1286 (2008).
7. Yang, S. N., Berggren, P. O. The eye as a novel imaging site in diabetes research. *Pharmacology, Therapeutics.* **197**, 103-121 (2019).
8. Schmidt-Christensen, A. et al. Imaging dynamics of CD11c(+) cells and Foxp3(+) cells in progressive autoimmune insulitis in the NOD mouse model of type 1 diabetes. *Diabetologia.* **56** (12), 2669-2678 (2013).
9. Berclaz, C. et al. Longitudinal three-dimensional visualisation of autoimmune diabetes by functional optical coherence imaging. *Diabetologia.* **59** (3), 550-559 (2016).
10. Nilsson, J. et al. Recruited fibroblasts reconstitute the peri-islet membrane: a longitudinal imaging study of human islet grafting and revascularisation. *Diabetologia.* **63** (1), 137-148 (2020).
11. Benninger, R. K., Piston, D. W. Two-photon excitation microscopy for the study of living cells and tissues. *Current Protocols in Stem Cell Biology.* **Chapter 4** Unit 4, pp. 11-24 (2013).
12. Goto, M. et al. Refinement of the automated method for human islet isolation and

presentation of a closed system for in vitro islet culture. *Transplantation.* **78** (9), 1367-1375 (2004).
13. Ewald, A. J., Werb, Z. Egeblad, M. Monitoring of vital signs for long-term survival of mice under anesthesia. *Cold Spring Harbor Protocols.* **2011** (2), pdb.prot5563 (2011).
14. Jansson, Carlsson, P. O. Graft vascular function after transplantation of pancreatic islets. *Diabetologia.* **45** (6), 749-763 (2002).
15. Konstantinova, I., Lammert, E. Microvascular development: learning from pancreatic islets. *Bioessays.* **26** (10), 1069-1075 (2004).
16. Fransson, M. et al. Mesenchymal stromal cells support endothelial cell interactions in an intramuscular islet transplantation model. *Regenerative Medicine Research.* **3**, 1 (2015).
17. Nyqvist, D. et al. Donor islet endothelial cells in pancreatic islet revascularization. *Diabetes.* **60** (10), 2571-2577 (2011).
18. Nair, G. et al. Effects of common anesthetics on eye movement and electroretinogram. *Documenta Ophthalmologica. Advances in Ophthalmology.* **122** (3), 163-176 (2011).
19. Iwasaka, H. et al. Glucose intolerance during prolonged sevoflurane anaesthesia. *Canadian Journal of Anaesthesia.* **43** (10), 1059-1061 (1996).
20. Hamilton, N. Quantification and its applications in fluorescent microscopy imaging. *Traffic.* **10** (8), 951-961 (2009).
21. Michelotti, F. C. et al. PET/MRI enables simultaneous in vivo quantification of beta-cell mass and function. *Theranostics.* **10** (1), 398-410 (2020).
22. Wang, P. et al. Monitoring of Allogeneic Islet Grafts in Nonhuman Primates Using MRI. *Transplantation.* **99** (8), 1574-1581 (2015).
23. Gotthardt, M. et al. Detection and quantification of beta cells by PET imaging: why clinical implementation has never been closer. *Diabetologia.* **61** (12), 2516-2519 (2018).
24. Joosten, L. et al. Measuring the Pancreatic beta Cell Mass in Vivo with Exendin SPECT during Hyperglycemia and Severe Insulitis. *Molecular Pharmaceutics.* **16** (9), 4024-4030 (2019).
25. Virostko, J. et al. Bioluminescence imaging in mouse models quantifies beta cell mass in the pancreas and after islet transplantation. *Molecular Imaging and Biology.* **12** (1), 42-53 (2010).

Figure 1

Click here to access/download;Figure;Figure 1a.psd

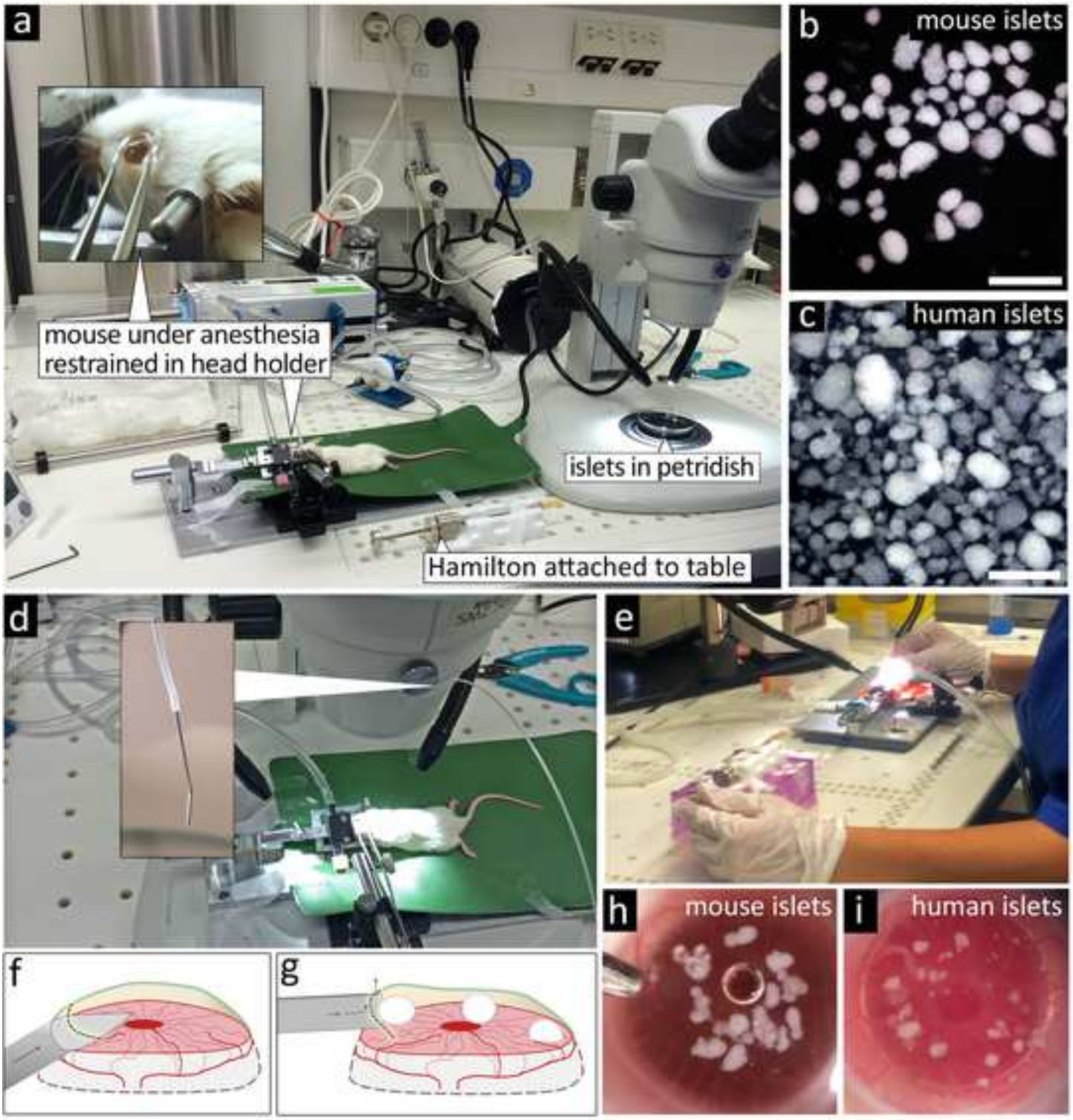

Figure 2

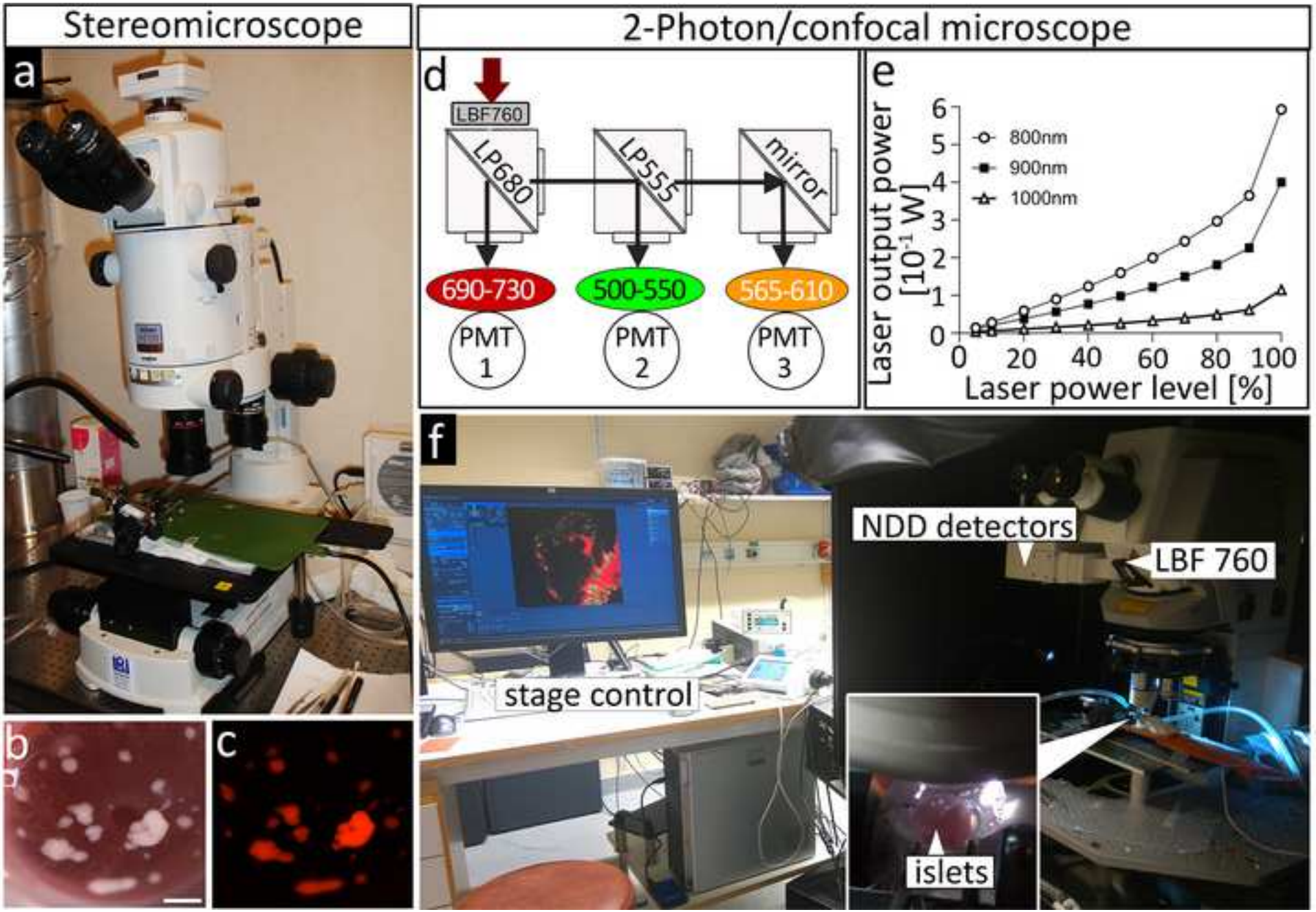

Figure 3

Click here to access/download;Figure;Figure 3a.psd

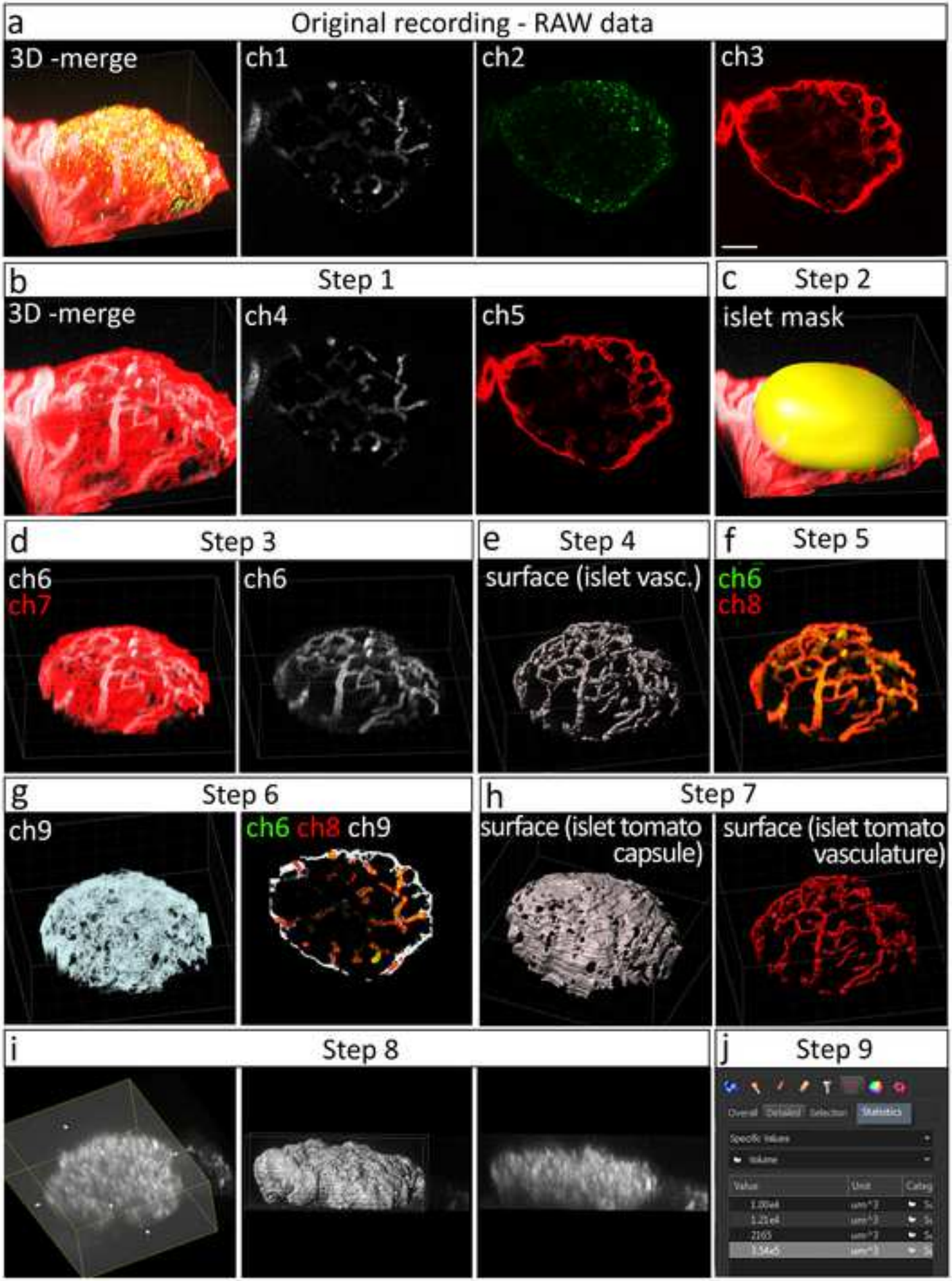

Figure 4

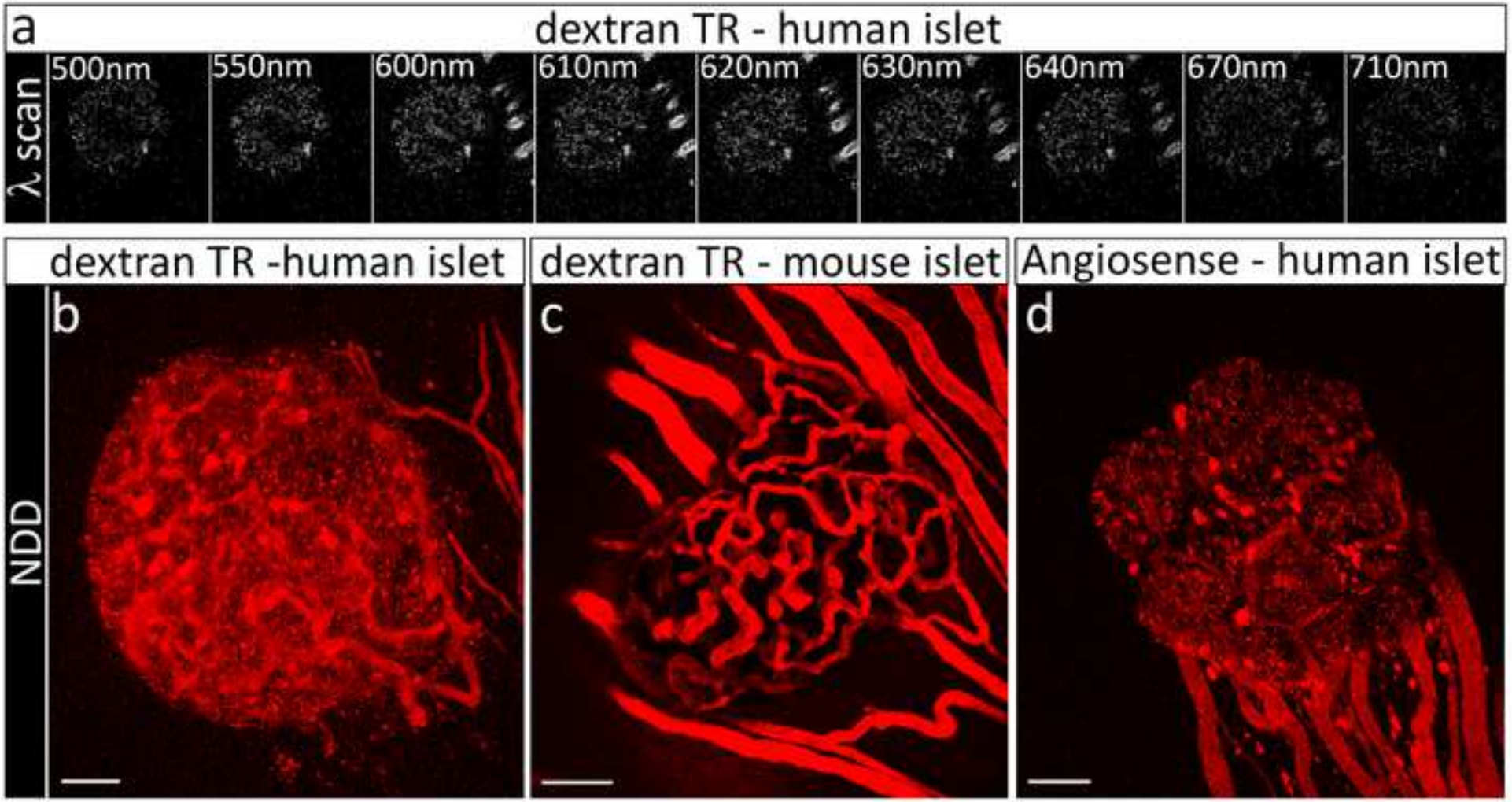

Figure 5

Click here to access/download;Figure;Figure_5a.psd

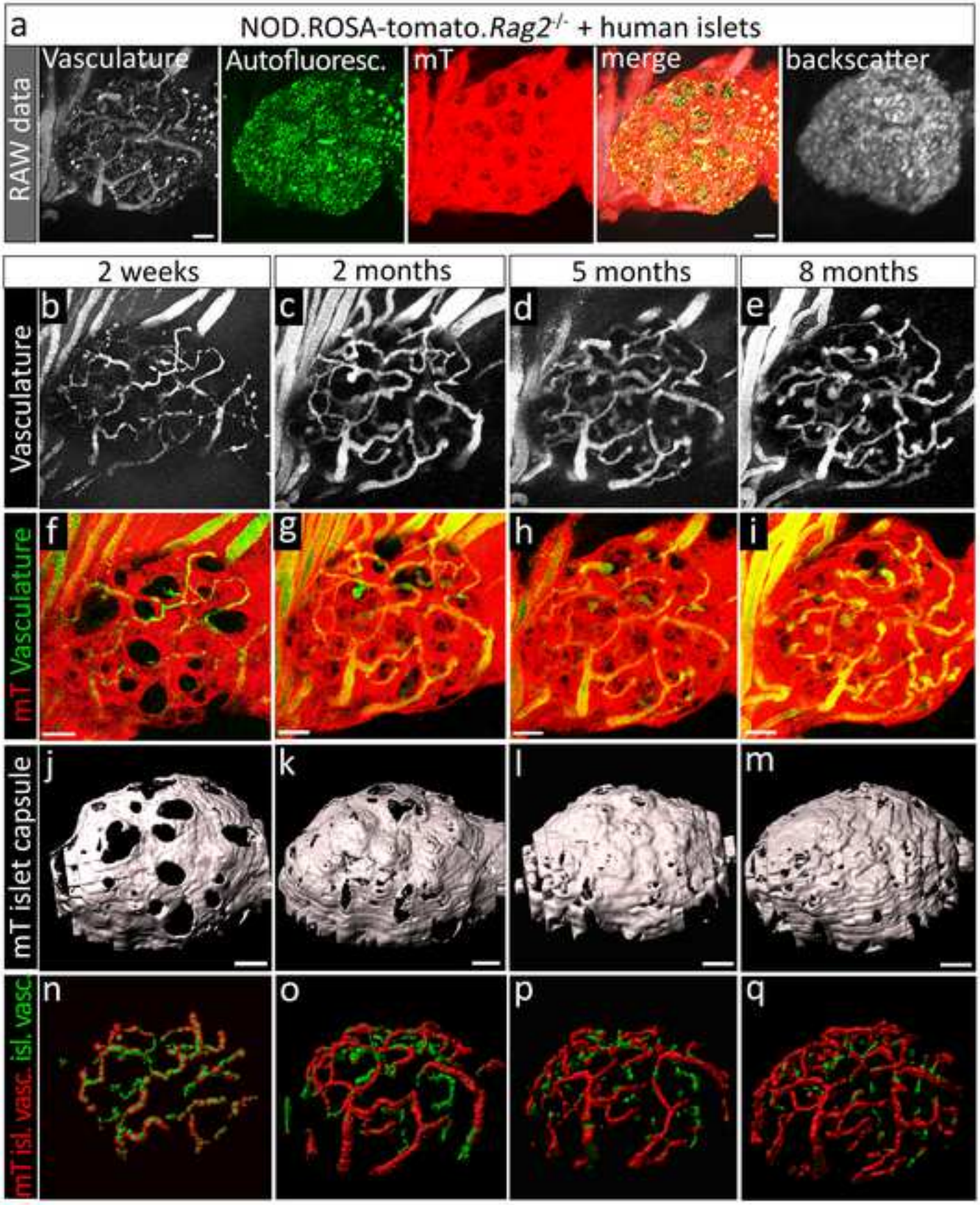

Name	Company	Catalog Number
Anasthesia machine, e.g. Anaesthesia Unit U-400	Agnthos	8323001
-induction chamber 1.4 L	Agnthos	8329002
-gas routing switch	Agnthos	8433005
AngioSense 680 EX	Percin Elmer	NEV10054EX
Aspirator tubes assemblies	Sigma	A5177-5EA
Buprenorphine (Temgesic) 0.3mg/ml	Schering-Plough Europé	64022
Capillary pipettes	VWR	321242C
Dextran-Texas Red (TR), 70kDa	Invitrogen	D1830
Eye cannula, blunt end , 25 G	BVI Visitec/BD	BD585107
Eye gel	Novartis	
Hamilton syringe 0.5 ml, Model 1750 TPLT	Hamilton	81242
Head holder		
-Head holding adapter	Narishige	SG-4N-S
-gas mask	Narishige	GM-4-S
-UST-2 Solid Universal Joint	Narishige	UST-2
-custom made metal plate for head-holder assembly		
-Dumont #5, straight	Agnthos	0208-5-PS
Heating pad, custom made		
Human islet culture media		
-CMRL 1066	ICN Biomedicals	
-HEPES	GIBCO BRL	
-L-glutamin	GIBCO BRL	
-Gentamycin	GIBCO BRL	
-Fungizone	GIBCO BRL	
-Ciproxfloxacin	Bayer healthcare AG	
-Nicotinamide	Sigma	
Image analysis software	Bitplane	
Image Aquisition software	Zeiss	

Infrared lamp	VWR	1010364937
Isoflurane Isoflo	Abott Scandinavia/Apotek	
Needle 25 G (0.5 x 16mm), orange	BD	10442204
Petri dishes, 90mm	VWR	391-0440
2-Photon/confocal microscope		
-LSM7 MP upright microscope	Zeiss	
-Ti:Sapphire laser Tsunami	Spectra-Physics, Mai Tai	
-long distance water-dipping lens 20x/NA1.0	Zeiss	
-ET710/40m (Angiosense 680)	Chroma	288003
-ET645/65m-2p (TR)	Chroma	NC528423
-ET525/50 (GFP)	Chroma	
-ET610/75 (tomato)	Chroma	
-main beam splitter T680lpxxr	Chroma	T680lpxxr
Polythene tubing (0.38mm ID, 1.09 mm OD)	Smiths Medical Danmark	800/100/120
Stereomicroscope	Nikon	
Stereomicroscope (Flourescence)		
-AZ100 Multizoom	Nikon	
-AZ Plan Apo 1x	Nikon	
-AZ Plan Apo 4x	Nikon	
-AZ-FL Epiflourescence with C-LHGFI HG lamp	Nikon	
-HG Manual New Intensilight	Nikon	
-Epi-FL Filter Block TEXAS RED	Nikon	
-Epi-FL Filter Block G-2A	Nikon	
-Epi-FL Filter Block B-2A	Nikon	
-DS-Fi1 Colour Digital Camera (5MP)	Nikon	
Syringe 1-ml, Omnitix	Braun	9161406V
Surgical tape	3M	

Comments/Description

used for isofluran anasthesia during surgery and imaging
connect via tubing to U-400
connect via tubing to U-400
imaging agent for injection, used to image blood vessels in human islet grafts
connect with pulled capillary pipettes for manual islet picking
fluid, for pain relief
used together with Aspirator tubes assemblies
imaging agent for injection
custom made from Tapered Hydrode lineator [Blumenthal], dimensions: 0.5 x 22mm (25G x 7/8in) (45^{o}), tip tapered to 30 G (0.3mm)
Viscotears, contains Carbomer 2 mg/g
Plunger type gas-tight syringe for islet injection

assemled onto metal plate

assemled onto metal plate

attached to UST-2 (custom made)
taped to the stereotaxic platform

cell culture media for human islets

Imaris 9
ZEN 2010

used to keep animals warm in the wake-up cage
fluid, for anesthesia
used as scalpel

Dichroic mirror to transmit 690 nm and above and reflect 440 to 650 nm size 25.5 x 36 x 1 mm
to connect with Hamilton syringe and eye canula
Model SMZ645, for islet picking
for islet graft imaging
wide field and long distance

contains EX540-580, DM595 and BA600-660
(EX510-560, DM575 and BA590)
(EX450-490, DM505 and BA520)

for Buprenorphine injection, used with 27 G needle

Dear Dr. Vineeta Bajaj,

We have now revised the manuscript accordingly as outlined below in the **point-to-point list**.

Please find enclosed:

- A response to the editor´s comments that responds to each point brought up

- A clean revised manuscript as ' 61234_R1_Manuscript ' file.

- A marked-up copy of the changes made from the previous article file as a '61234_R1_Revised Manuscript with Track Changes' file.

Yours sincerely

Anja Schmidt-Christensen

Point-to point list:

Editorial comments:

1. The editor has formatted the manuscript to match the journal's style. Please retain.

Authors response: retained as requested

2. Please address specific minor comments marked in the manuscript.

2.1. Please proofread the manuscript
Authors response: completed as requested.

2.2. line 100, How do you visually identify exocrine tissue?

Authors response: The sentence "Exocrine tissues appears translucent." was added.

2.3. line 115, Reworded please check.
Authors response: editorial change is accepted by the author.

2.4. line 148, Added here. Please check.

Authors response: editorial change is accepted by author.

2.5. line 195, Any specific volume?

Authors response: The additional NOTE was added to that paragraph "NOTE: Aim for an injection volume of 3 µl - 8 µl. A too large volume will expose the eye to unnecessarily high intraocular pressure and may result in reflux of the injected islets out of the anterior chamber."

2.6. line 220, Please include a note stating after how much time do you perform the imaging?

Authors response: following NOTE was added to the section: "NOTE: Taking overview images of the eye prior 2-Photon imaging is recommended to localize islets of interest. This can be accomplished by using a (fluorescence) stereoscopic microscope (Figure 2a-c) from earliest 4-5 days after transplantation. Avoid restraining the eye too tightly at this early time point after transplantation. Proceed to 2-Photon imaging from 6-7 days post transplantation."

2.7. line 227, Please ensure that this is present in the table.

Authors response: the "image acquisition software" was added to Materials

2.8. line 227-230, Please reword for clarity.

Authors response: completed as requested.

2.9. line 242, Please include a step to show that mice was secured on the head holder for microscopy.

Authors response: the phrase "…, transfer to the head holder platform…" was added.

2.10. line 296, Please adjust the numbering of the Protocol to follow the JoVE Instructions for Authors. For example, 1 should be followed by 1.1 and then 1.1.1 and 1.1.2 if necessary

Authors response: section 7 was reformatted as requested

2.11. line 449, Please expand MIP

Authors response: completed as requested

2.12. Figure legends, Please include scale bar.

Authors response: scale bars were included in all figures requested.

2.13. Figure legends, Please mark it as a, b, c panels to have similar numbering styles as other figures. When referring the figures in the protocol, please ensure that the figures are referred in the order of their numbering. So figure 1 and 2 will be cited before Figure 3

Authors response: Figures were reordered and renamed as requested

2.14. Materials table, Please sort the table in alphabetical order remove trademark (™) and registered (®) symbols.

Authors response: completed as requested

3. Please reword lines 59-60, 63-66, 382-386, 539-546, 555-562.

Authors response: completed as requested